1630 *KSME International Journal, Vol. 15, No. 12, pp. 1630~1638, 2001*

On the Contact of Partial Rotor Rub with Experimental Observations

Yeon-Sun Choi*

School of Mechanical Engineering, Sungkyunkwan University, Suwon, Kyunggi-do 440-746, Korea

Partial rotor rub occurs when an obstacle on the stator of a rotating machinery disturbs the free whirling motion of the rotor, which is more common than full annular rub among the cases of rubbing in rotating machinery. The intermittent contacts and friction during partial rotor rub makes the phenomenon complex. The several nonlinear phenomena of superharmonics, subharmonics, and jump phenomenon are demonstrated for the partial rub using an experimental apparatus in this study. The orbit patterns are also measured experimentally. In order to explain the phenomena of partial rotor rub, the analytical model for the contact between the rotor and stator should be chosen carefully. In this respect, a piecewise-linear model and a rebound model using the coefficient of restitution are investigated on the basis of the experimental observations. Also, Numerical simulations for the two models of contact are done for the various system parameters of clearance, contact stiffness, and friction coefficient. The results show that the piecewise-linear model for partial rotor rub is more plausible to explain the experimental observations.

Key Words : Partial Rotor Rub, Jump Phenomenon, Coefficient of Restitution, Piecewise-Linear, Contact Stiffness, Friction Coefficient

1. Introduction

During the whirling motion of a rotor, the rotor comes to contact with the stator. The contact between the rotor and stator during whirling motion is called rubbing. The rubbing generated by some perturbation of normal operating conditions of a machine can maintain itself, becomes more severe, and leads to a higher vibration level.

Because of this disastrous phenomenon, many researchers have investigated for the safe and reliable design of rotating machinery. Black (1968) is a notable contributor to this problem. He tried to explain the physics of rubbing using the polar receptance of the rotor and stator. Choy and Padovan (1987) performed a numerical analysis to yield insights as to the interrelationship between rub force histories, energy levels, rub duration, incidence separation angles, and backward whirl initiation. Choi and Noah (1987) treated this problem as a piecewise linear vibration problem, and proposed an algorithm to calculate the steady-state solution using the FFT technique. The results showed that superharmonic and subharmonic responses could be found due to rubbing. Crandall and Lingener (1990) showed a very specific pattern of whirling frequency responses during rubbing by an experiment, and developed a theory to explain backward rolling and backward slipping for the case of full annular rub. The study of full annular rub has been done more than the study of partial rotor rub, since the circumferential homogeneity of full annular rub makes the problem easy and simple. However, partial rotor rub is more common in practice. Intermittent impacts and friction during partial

E-mail : yschoi@yurim.skku.ac.kr
TEL : +82-31-290-7440; **FAX** : +82-31-290-5849
School of Mechanical Engineering, Sungkyunkwan University, Suwon, Kyunggi-do, 440-746, Korea.
(Manuscript **Received** February 27, 2001; **Revised** September 1, 2001)

rotor rub make the phenomenon complex. In this respect, Beatty (1985) suggested a reliable rubbing detection methodology by the magnitudes between relative harmonic frequencies for the case of partial rotor rub. Both theoretical and experimental investigations were carried out by Muszynska (1984) on the partial rotor rub. Steady-state subharmonic vibrations of the order of 1/2, 1/3, 1/4, etc. were presented in her paper. And she also demonstrated complex orbit patterns experimentally for a heavy rub and analyzed them theoretically. Xingjian (1999) investigated the nonlinear vibration of partial rotor rub with a motion stopper by numerical and experimental methods. Xingjian used a model with the combination of the Coulomb friction and piecewise linear spring, and observed a chaotic vibration in the rotor/stopper rubbing experiments. Choi (2000) demonstrated partial rotor rub phenomenon in the laboratory using an experimental apparatus to show the different orbit patterns between light and heavy rub. Also, the phenomenon of one impact per two rotations during heavy rub, which demonstrates the occurrence of subharmonic response, is discussed experimentally and numerically.

Most researches related to the contact problem in mechanical systems preferred numerical simulation under the assumption of a piecewise-linear model or of a rebound model using the coefficient of restitution. However, the contact model should be chosen carefully for the investigation of nonlinear dynamic phenomenon of the system. The analysis on rotor rub is generally done numerically using a piecewise-linear model or a rebound model. The exactness of the models for contact cannot be confirmed without the comparison with the experimental results. In this respect, the comparisons of the contact models on the basis of experimental observations for the case of partial rotor rub are done in this paper. Contact stiffness, the coefficient of restitution, and friction coefficient for the contact during partial rotor rub are calculated from the comparison between the numerical simulation and the experimental results. Also, the numerical simulations for the model of partial rotor rub are done for the various system parameters of clearance, contact stiffness, and friction coefficient.

2. Analytical Model

The experimental apparatus of Fig. 1 was set up in order to investigate partial rotor rub. The contact between the rotor and stator was supposed to occur at the center of the shaft. The whirling of the rotor motion was measured at the center of the shaft just near the contact point, using gap sensors in vertical and horizontal directions, respectively. When the runout of the rotor due to the unbalance or bend of the shaft comes to the limit of the given clearance, the shaft comes into contact with a protrusion on the stator. The orbit of the rotor due to the contact with the protrusion would not be a circular shape. The contact between the rotor and stator causes the variation of stiffness of the rotor, and the friction at the contact surface makes complex whirling orbits. For the analysis of the partial rotor rub, an analytical model of Fig. 2 is assumed. Where G is the center of rotor mass, O_S and O_B are the shaft center and the center of two end bearings, respectively. And the equations of motion (1) and (2) are derived for the x and y direction each.

$$m\ddot{x}+c\dot{x}+kx+f=me\omega^2\cos\omega t \quad (1)$$

$$m\ddot{y}+c\dot{y}+ky+N=me\omega^2\sin\omega t \quad (2)$$

m, c, and k are the rotor mass, damping coefficient and stiffness coefficient. e and ω are the rotor eccentricity and exciting frequency, i.e., the rotor speed. N and f are the normal and tangential forces, which characterize the physics of the contact mechanism during rubbing. The contact has generally been modeled using a piecewise-linear model or a rebound model using the coefficient of restitution. The normal and tangential forces can be stated in the piecewise-linear model as below.

$$N=\begin{cases} K_c(y-d) & : y>d \\ 0 & : y\le d \end{cases} \quad (3)$$

$$f=\begin{cases} \mu N & : y>d \\ 0 & : y\le d \end{cases}$$

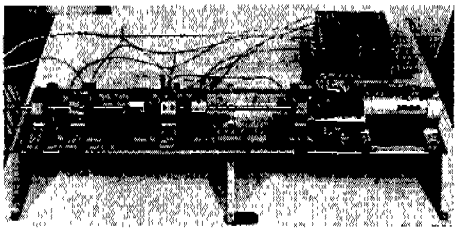

Fig. 1 Experimental apparatus of RK-4 rotor kit

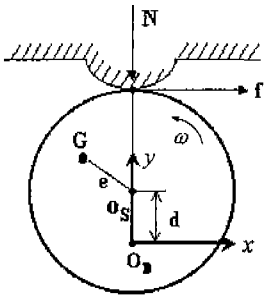

Fig. 2 Analytical model for partial rotor rub

μ is the friction coefficient between the rotor and stator, while K_c is the contact stiffness of a protrusion. It is assumed that there is a clearance of d between the rotor and stator in the y direction as shown in Fig. 2. Since the period of impact is very short, the damping during contact can be neglected, and only the elasticity for the deformation of the protrusion will be considered in our analysis as a contact stiffness. Also, the Coulomb type friction is assumed only in the x direction.

In contrast, the rebound model assumes that the normal and tangential forces are both zeros. Instead, at the contact point, there is a velocity change with the ratio of the coefficient of restitution given by :

$$\dot{y}_- = -\nu \dot{y}_+ \tag{4}$$

where ν is the coefficient of restitution and $\dot{y}_+$ means the velocity before the contact and $\dot{y}_-$ for after the contact.

The equations of the piecewise-linear model or the rebound model cannot be solved without the exact values of characteristic parameters; K_c, μ, and ν, which are very difficult to obtain in practice. In this respect, an experiment should be done for the analysis and for the determination of the contact model. The system parameters should be found from the calculations for the experimental data.

3. Experimental Apparatus

In this research, the RK-4 rotor kit, manufactured by Bently Nevada Co. as shown in Fig. 1 was used to demonstrate various partial rubbing phenomena. The contact between the rotor and stator was accomplished by making a protrusion consisting of a brass screw bolt at the top of the stator which is at the center of the shaft. When the runout of the rotor exceeds the given clearance between the protrusion and shaft during the whirling motion of the rotor, the shaft comes into contact with the protrusion. The whirling orbit was measured using two gap sensors at the center of the shaft in the x and y direction, respectively. The running speed of the rotor was measured by a photosensor. The signals measured by the gap sensors were stored in a computer through analog-to-digital conversion, and analyzed using the MATLAB software. The natural frequency and damping coefficient of the rotor system were measured by an impact test and a rotor running test without the brass screw bolt at the stator. An impact was exerted on the center of the shaft, where the contact happens, and the response was measured using the gap sensors. The free run test means a running test for the rotor kit by increasing and decreasing the speed of the rotor. Since the tests were done after the cautious adjustment of the rotor kit, the orbit of the rotor became circular. It is very difficult to obtain the circular orbit in this experiment since the homogeneity of the system parameters in the vertical and horizontal direction is not normally guaranteed. The stiffness of the shaft was found by the static deflection test, which measures the static deflection of the shaft when a force is exerted on the center of the shaft. The mass of the rotor was calculated from the natural frequency and stiffness of the shaft. The eccentricity of the rotor was calculated from the response curve of the rotor running test. Several experiments and calculations result in the system parameters of the

Table 1 System parameters of the rotor

Parameters	Units	Values
mass, M	kg	1.25
damping, C	kg/s	8.5
stiffness, K	N/mm	35
eccentricity, e	mm	0.036

rotor kit as shown in Table 1.

4. Runout and Whirling Orbit

After the careful set-up of the rotor kit, running operations were done for various clearance sizes between the rotor and stator with increasing and decreasing rotor speeds. The clearance size was set-up by adjusting the bolt screw and measured using a thickness gauge. The overall vibration levels for different clearance sizes are shown in Fig. 3(a) and 3(b) for the x and y directions, respectively. The magnitude of the responses means a peak-to-peak of the displacement in each direction. As a result, some amplitudes in Fig. 3 can exceed the clearance sizes. The graphs labeled as "no rub" denote the responses without the brass screw bolt which restricts the whirling motion of the rotor. As shown in Fig. 3(a), there are small variations in the magnitude of the responses in the x direction as the clearance size changes. However, the magnitude of the y direction response of Fig. 3(b) decreases as the clearance becomes smaller. Near the critical speed range of 1600rpm, the maximum amplitude exceeds the clearance size. This means that the center of the shaft during rubbing moves to a lower position as the orbit becomes larger ever though it is not shown in Fig. 4. Figure 4 is drawn by the AC components of the response to clarify the orbital shapes. In the case when the rotor speed decreases, as shown in Fig. 3(c), the y direction responses in the range of above the critical speed are smaller than those of increasing speed of Fig. 3(b), which indicates the jump phenomenon due to the nonlinearity of hardening stiffnees.

Figure 4 shows the whirling orbits during partial rotor rub for 0.1 mm and 0.5 mm clearance

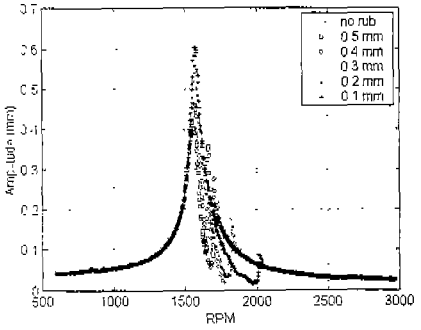

(a) X-axis response for increasing rotor speed

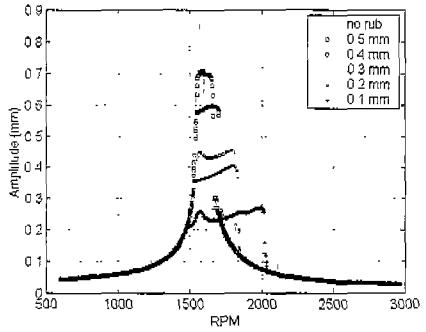

(b) Y-axis response for increasing rotor speed

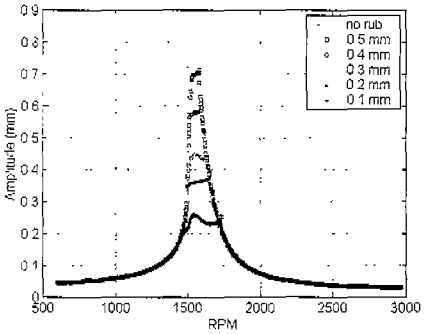

(c) Y-axis response for decreasing rotor speed

Fig. 3 Experimentally observed vibration level

sizes near the range of the critical speed. The variation of orbit patterns for the case of 0.5 mm clearance is shown in Fig. 4(a) as the rotor speed increases and in Fig. 4(b) as the rotor speed decreases. Far below and above the critical speed, the orbits are almost circles. However, it draws an elliptical or a distorted orbit in the range of the critical speed. Also, the orbit shape at each rotor speed differs depending on whether the rotor speed increases or decreases. The orbit at the 1670 rpm in Fig. 4(a) shows multiple orbits. It is

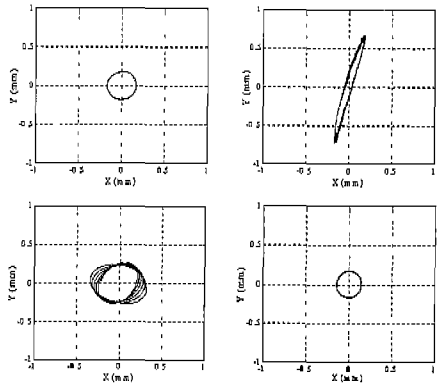

(a) 0.5mm clearance during increasing (1460, 1610, 1670, 1760rpm)

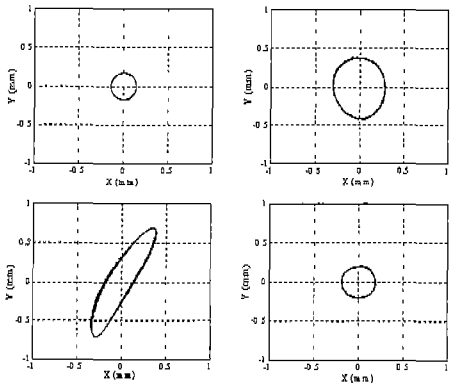

(b) 0.5mm clearance during decreasing (1760, 1640, 1550, 1460rpm)

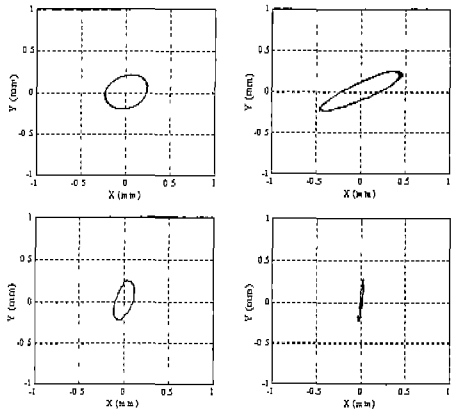

(c) 0.1mm clearance during increasing (1500, 1600, 1750, 1900rpm)

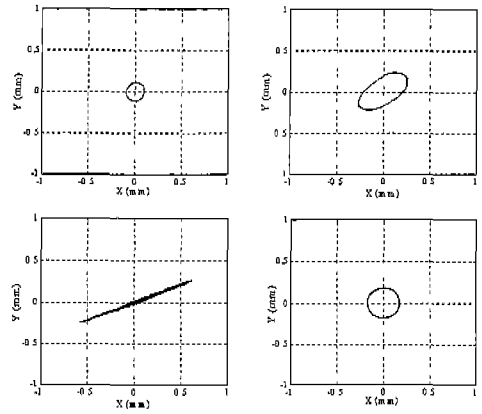

(d) 0.1mm clearance during decreasing (1850, 1650, 1550, 1450rpm)

Fig. 4 Experimentally observed orbits

believed that the response at the 1670 rpm is a transient or an unstable one since the rotor speed is gradually increased during the experiment.

For the case of 0.1 mm clearance as shown in Fig. 4(c) and 4(d), the elliptical orbit starts at lower rotor speed than in the 0.5 mm clearance case, and it has an inclination, but after the range of the critical speed the orbit becomes a vertical line for the case of increasing rotor speed. The comparison between Fig. 4(c) and Fig. 4(d) shows different orbit shapes even in the range of equal rotor speed, which is believed due to the influence of nonlinearities, which comes from the contact and friction during rubbing.

5. Rebound Model

The coefficient of restitution is commonly used for the investigations of the collision problems in mechanical engineering. Basically the adoption of the coefficient of restitution assumes the system having an infinite stiffness and finite damping. The rebound model using the coefficient of restitution can be applied to calculate the response of partial rotor rub. Figure 5 shows the calculated responses of the partial rotor rub with the comparison of the experimental results. The calculation procedure is based on the Runge-Kutta algorithm that incorporates Eq. (4), which

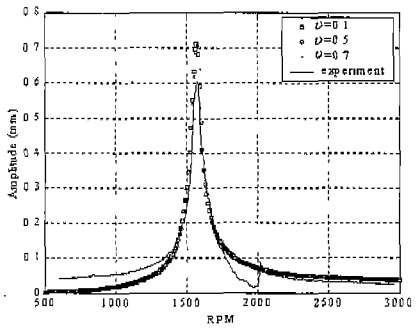

(a) X-axis response during increasing

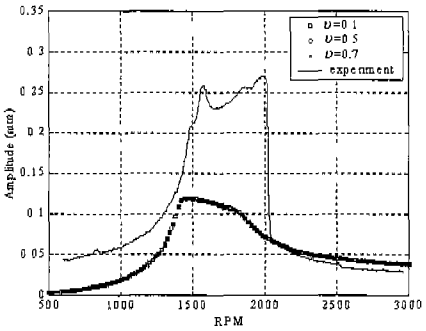

(b) Y-axis response during increasing

Fig. 5 Vibration level for rebound model

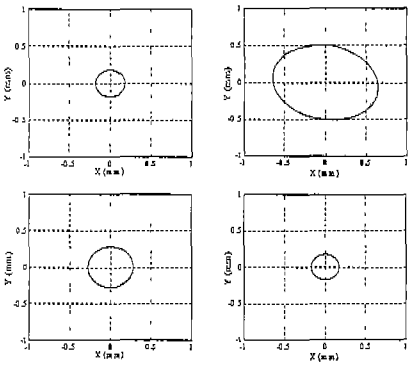

(a) 0.5mm clearance during increasing (1460, 1550, 1610, 1700rpm)

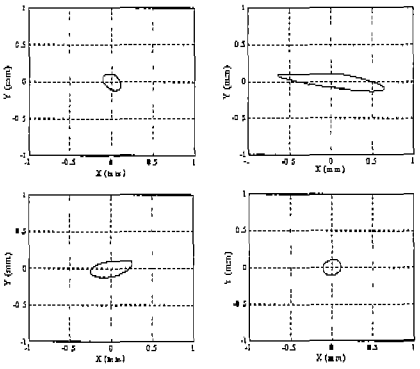

(b) 0.1mm clearance during increasing (1400, 1550, 1650, 1800rpm)

Fig. 6 Calculated orbits for rebound model

models the contact as an abrupt changes in velocity with a ratio equal to the coefficient of restitution. From the definition of the coefficient of restitution, the velocity changes are applied only in the y direction. As shown in Fig. 5, the calculated x responses coincide well with the experimental results except in the region below the critical speed. However, there are large differences in the y response, especially in the region of critical speed. The differences in the region below the critical speed, are believed due to the bearing clearance of 0.05 mm. The phase angles of the response of the rotor below the critical speed are almost zero. The zero phase angle means that the response is the sum of the real response and the bearing clearance, which is not included in the numerical simulation. In the region above the critical speed, the phase angle goes to π, which can neglect the bearing clearance in its response. Accordingly, the calculated responses in that region show good agreement with the experimental results. As shown in Fig. 5 the different coefficient of restitution does not result in the change of the vibration level in x and y directions. Therefore, it is believed that the values of the coefficient of restitution are not critical to decide the magnitude of the responses. Figure 6 shows the calculated orbits with the coefficient of restitution of 0.1 for different rotor speeds. It shows almost a circle or a distorted ellipse. The calculated orbits of 1550 and 1650 rpm for the case of 0.1mm clearance show horizontally flat shapes, which are limited by the protrusion. The comparison with the experimentally observed orbits in Fig. 4 shows that the coefficient of restitution can calculate approximately the magnitude of runouts. However, the rebound model is not correct one for the calculation of the orbits of the partial rotor rub.

6. Piecewise-Linear Model

The piecewise-linear model of Eq. (3) is commonly used for the numerical simulation of rotor rubbing problem. Figures 7~9 are the results of the numerical simulation to find the parameters of the piecewise-linear model for partial rotor rub with the experimental results. The numerical simulations were done by the Runge-Kutta method for Eq. (1), (2), and (3).

Figure 7 shows the peak-to-peak response in the x and y directions with the variation of contact stiffness for the case of 0.1mm clearance. There are also the differences between the results of the numerical simulation and those of the experiment in the region below the critical speed which can also be explained by the existence of the bearing clearance. The contact stiffnesses in Fig. 7 are designated by the times of the shaft stiffness of the rotor kit. The contact stiffness K_c, which is the 2000 times of the shaft stiffness, results in the closest responses to the experimental results especially in the vertical responses as shown in Fig. 7. The factor of 2000 is almost the same as the bar stiffness of the brass ball screw, which is calculated from the Young's modulus multiplied by the area and divided by the length of the ball screw. Accordingly the factor of 2000 can be physically acceptable. The factors less than 2000 for the contact stiffness result in fairly good agreements in the range of the critical speed but mismatch above the critical speed for the x responses, and brings the diverging responses for the y direction as the rotor speed increases, which needs more study on the view point of dynamic stability.

Figure 8 shows the effect of eccentricity during partial rotor rub for the case of 0.1mm clearance. Generally, larger eccentricity values result in larger the x and y responses. However, 0.06mm eccentricity brings a diverging response near the critical speed as shown in Fig. 8(b). This

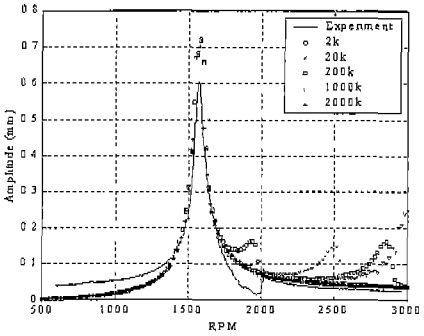

(a) X-axis response during increasing

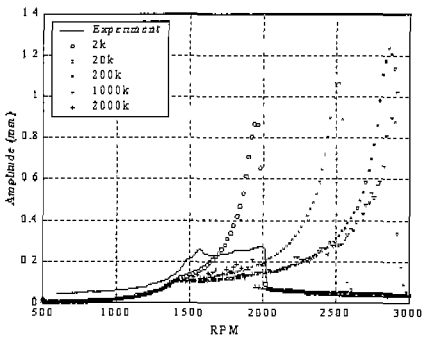

(b) Y-axis response during increasing

Fig. 7 Effect of contact stiffness in piecewise-linear model (e=0.036mm, μ=0.1)

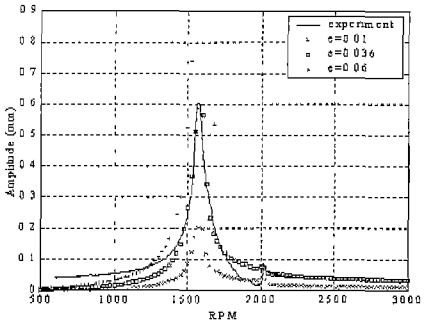

(a) X-axis response during increasing

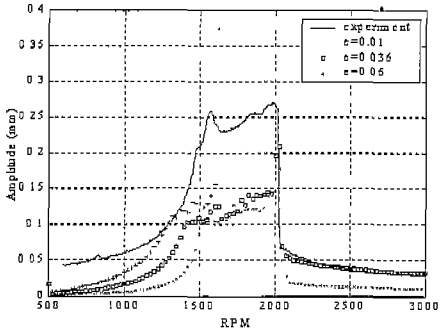

(b) Y-axis response during increasing

Fig. 8 Effect of eccentricity in piecewise-linear model (K_c=2000k, μ=0.1)

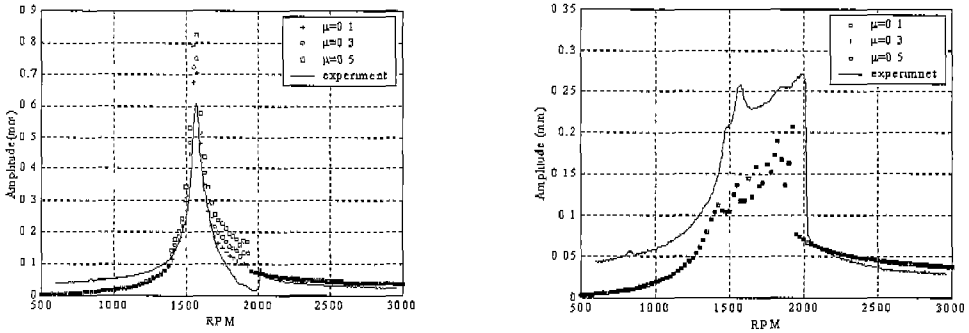

(a) X-axis response during increasing (b) Y-axis response during increasing

Fig. 9 Effect of friction coefficient in piecewise-linear model (K_c=2000k, e=0.036mm)

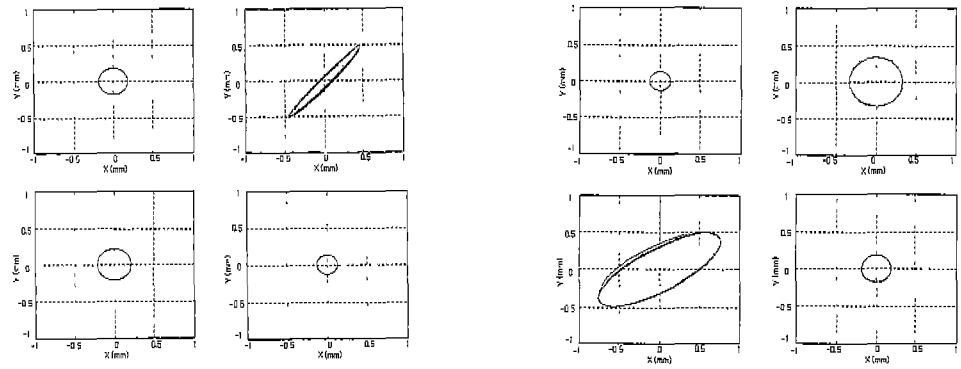

(a) 0.5mm clearance during increasing (1460, 1610, 1670, 1760rpm)

(b) 0.5mm clearance during decreasing (1760, 1640, 1550, 1460rpm)

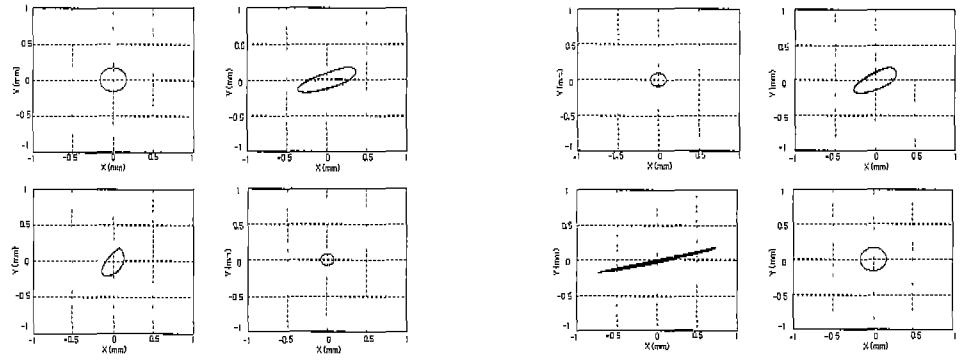

(c) 0.1mm clearance during increasing (1500, 1600, 1750, 1900rpm)

(d) 0.1mm clearance during decreasing (1850, 1650, 1550, 1450rpm)

Fig. 10 Calculated orbits for piecewise-linear model

indicates that the rotor response with partial rotor rub can go to unstable one for a larger eccentricity, which may lead to a chaotic response. Figure 9 shows the effects of the friction coefficient for the case of 0.1 mm clearance. Larger friction coefficients result in larger responses in the horizontal direction, but almost negligible effect on the vertical direction. From this result, the assumption that the friction acts only in x direction in Eq. (1) and (3) seems to be

correct. The orbits calculated for the piecewise-linear model are shown in Fig. 10 for increasing and decreasing the rotor speeds for the cases of 0.5 mm and 0.1 mm clearance, respectively. Comparisons between the calculated orbits and the experimentally observed ones in Fig. 4 shows that the piecewise-linear model is plausible to model the partial rotor rub not only for the magnitudes of responses but also for the orbit shapes. An inclined ellipse and a folded ellipse are shown in the numerical simulations as were observed from the experiment. Especially for the case of 1900 rpm in 0.1 mm clearance shown in Fig. 4(c) and Fig. 10(c), there is a completely different orbit, which shows the possibility of the existence of multiple responses in partial rotor rub. It was shown in the results of the numerical simulations and in those of the experiment that there are abrupt changes in orbit shapes as the rotor speed increases or decreases, which shows the possibility of a bifurcation due to its nonlinearity in partial rotor rub.

7. Conclusion

Partial rotor rub due to the contact with a non-rotating obstacle is investigated experimentally and analytically to understand the rubbing phenomenon and to model the responses analytically. The rubbing phenomena are demonstrated using the RK-4 rotor kit of Bently Nevada Co. The experiment and its analysis show the following results.

(1) Most orbits shown in the experiment were simple ones even though strong nonlinearities are involved due to the contact and friction.

(2) The piecewise-linear model is better than the rebound model using the coefficient of restitution to modeled the partial rotor rub not only for the vibration level but also for the orbit shapes.

(3) The responses of partial rub show a typical nonlinear response of the jump phenomenon due to hardening spring effect.

(4) The friction coefficient influences only the tangential response, while the contact stiffness influences only the normal response. Therefore, larger friction coefficient result, in larger responses in the horizontal direction but almost negligible effect on the vertical direction.

(5) The rebound model can calculate approximately the magnitude of runouts. However, the model is not enough to simulate the orbit of partial rub.

Acknowledgements

This work was supported by a grant from the Critical Technology 21 Project of the Ministry of Science and Technology, Korea, which is gratefully acknowledged.

References

Beatty, R. F., 1985, "Differentiating Rotor Response Due to Radial Rubbing," *Journal of Vibration, Acoustics, Stress, and Reliability in Design*, Vol. 107, pp. 151~160.

Black, H. F., 1968, "Interaction of a Whirling Rotor with a Vibrating Stator across a Clearance Annulus," *Journal of Mechanical Engineering Science*, Vol. 10, pp. 1~12.

Choy, F. K. and Padoban, J., 1987, "Nonlinear Transient Analysis of Rotor-Casing Rub Events," *Journal of Sound and Vibration*, Vol. 113, No. 3, pp. 529~544.

Choi, Y.-S. and Noah, S. T., 1987, "Nonlinear Steady-State Response of a Rotor-Support System," *Journal of Vibration, Acoustics, Stress, and Reliability in Design*, Vol. 109, No. 4, pp. 225~261.

Choi, Y.-S., 2000, "Experimental Investigation of Partial Rotor Rub," *KSME International Journal*, Vol. 14, No. 11, pp. 1250~1256.

Crandall, S. H. and Lingener, A., 1990, "Experimental Investigation of Reverse Whirl of a Flexible Rotor," *ITFoMM Third International Conference on Rotordynamics*, Lyon, France, pp. 13~18.

Muszynska, A., 1984, "Partial Lateral Rotor to Stator Rubs," *ImechE* C281/84, pp. 327~335.

Xingjian, D., Xiaozhang, Z., and Zhaoxiong, J., 1999, "On the Vibration of Rotor With Rotor/Stopper Rubbing," DETC99/VIB-8 274, *ASME, 17th Biennial Conference on Mechanical Vibration and Noise.*